

## Effect of intergrain junctions and flux pinning on transport critical currents in $\text{YBa}_2\text{Cu}_3\text{O}_{7-\delta}$ granular superconductors

J. Jung and I. Isaac

*Department of Physics, University of Alberta, Edmonton, Alberta, Canada T6G 2J1*

M. A-K. Mohamed

*Department of Physics, University of Lethbridge, Lethbridge, Alberta, Canada T1K 3M4*

(Received 6 October 1992; revised manuscript received 8 April 1993)

Studies of the dependence of the intergrain critical currents on temperature (60–90 K) and magnetic field (0–100 G) were performed for samples of  $\text{YBa}_2\text{Cu}_3\text{O}_{7-\delta}$  ceramics (YBCO) and of a 2-wt.% Ag-doped  $\text{YBa}_2\text{Cu}_3\text{O}_{7-\delta}$  composite (YBCO-Ag). The measurements were done using ceramic rings in a persistent mode and a scanning cryogenic Hall probe. This technique allowed us to satisfy conditions not available in the studies of critical currents before. A self-sustaining supercurrent (sensitive to any resistive dissipation) was used to detect the intergrain critical current  $I_c$ . Its magnitude and relaxation were measured using a contactless method (a Hall probe). The results of the measurements of  $I_c$  on temperature close to the intergrain  $T_c^*$  confirmed the presence of the superconductor-insulator-superconductor tunnel intergrain junctions in YBCO and the superconductor-normal-metal-superconductor proximity junctions in YBCO-Ag. For YBCO, the  $I_c(T) = \text{const}(1 - T/T_c^*)$  dependence is not affected by the applied magnetic field, however, for YBCO-Ag the  $I_c(T) = \text{const}(1 - T/T_c^*)^2$  dependence is not preserved, suggesting a strong effect of magnetic flux creep on critical currents. The intergrain  $T_c^*$  is about 5 K lower than the intragrain  $T_c$  and about 4 K lower than the “zero-resistance  $T_c$ ” measured using a conventional  $I$ - $V$  technique. Dissipation of a persistent current measured in the YBCO-Ag ring provided strong evidence that the transport current is controlled by an intergrain flux creep with the energy barrier proportional to  $I_c$ . The results revealed that the intergrain critical current density  $J_{cT}$  in YBCO-Ag has lower values than  $J_{cT}$  of YBCO, and the observed higher total critical currents are due to a larger surface area of grain-boundary conduction in this composite.

### I. INTRODUCTION

The transport and magnetic properties of superconducting Y-Ba-Cu-O (YBCO) ceramics or polycrystalline oriented thin films are affected by grain boundaries present in those materials. At low magnetic fields up to 200–300 G grain boundaries in ceramic YBCO behave like junctions between weakly coupled superconducting grains.<sup>1–3</sup> At higher fields weak links are decoupled but there still exists a second non-weak-linked component of intergrain conduction which is not decoupled by the magnetic field. This component is believed to arise from regions of strong conduction within each grain boundary such as microbridges of intrinsic intragranular material.<sup>4</sup> Studies on aligned bulk polycrystalline YBCO (Ref. 4) showed that the fraction of a non-weak-linked material is enhanced by grain alignment but still only 0.01–0.1% of the grain-boundary area is occupied by strongly linked microbridges. Therefore, weak links are responsible for low critical current density  $J_c$  and the extreme sensitivity of  $J_c$  to small magnetic fields. In spite of intensive studies of grain boundaries in YBCO, there are still several problems, crucial for the understanding of their superconducting properties which remain unsolved.

The first one concerns the intrinsic nature of superconducting weak links. It is unclear whether the intergrain junctions are the superconductor-insulator-super-

conductor (SIS)-type Josephson tunnel junctions or the superconductor-normal-metal-superconductor (SNS)-type Josephson (DeGennes) proximity junctions. Related to that is the question what is the mechanism by which the Ginzburg-Landau order parameter (which is equivalent to the density of Cooper pairs or to the amplitude of the pair wave function) is suppressed at the grain boundary. Resolving these questions could help to explain to what extent the low critical current densities of YBCO ceramic samples are related to the intrinsic characteristics of grain boundaries.

The second problem concerns magnetic-field effects on critical current of intergrain junctions. While it was well documented that the intragrain  $J_c$  is controlled by the intragrain flux creep, no evidence was provided for an intergrain flux-creep-controlled transport current. The additional problem is to distinguish between the current limiting behavior of grain boundaries in low magnetic fields and the changes in the transport current caused by the intergrain flux trapping and depinning. The measurements that are necessary for proper characterization of those effects include the dependence of the transport critical current  $I_c$  on temperature for various magnetic fields and the dependence of  $I_c$  on magnetic fields for various temperatures. The essential experimental condition is to measure the real response of  $I_c$  to changing temperature or magnetic field. This is especially important at temper-

atures close to  $T_c$ . However, many experimental methods that were used to estimate the transport critical current density do not satisfy that requirement. The techniques widely applied to high- $T_c$  ceramics and films for that purpose are (1) the  $I$ - $V$  four-probe technique<sup>5-11</sup> or (2) the ac magnetic induction method.<sup>12-14</sup> There are several reasons that make those two methods unreliable.

The problem with the  $I$ - $V$  method is the Joule heating at the contacts and the value of minimum resistance, that can be measured usually in a range of about  $10^{-7}$ - $10^{-5}$  ohm. The latter is related to sensitivity of instruments and to a voltage (or an electric field) criterion of 0.1-2  $\mu$ V (1-10  $\mu$ V/cm) used to define the critical current. As a consequence, this method does not make a clear distinction between very low resistance and superconductivity. Its insensitivity to a resistive dissipation of supercurrent at temperatures close to  $T_c$  seems to be the main reason for the observed discrepancy in the  $I_c$  vs temperature dependence reported by different groups for ceramic or thin-film high- $T_c$  materials.

The ac induction technique, on the other hand, uses ac susceptibility measurements and critical state model (Bean's critical state equation) to estimate critical currents. According to the Bean's critical state model,<sup>15</sup> superconducting samples respond to the external magnetic field with shielding currents that flow at the level of critical current density  $J_c$ . In the case of ceramic samples diamagnetic shielding consists of two components: intergrain and intragrain ones. At low magnetic fields, superconducting ceramic samples exhibit strongly nonuniform distribution of intergrain shielding supercurrents because of the magnetic interaction between shielding current loops and demagnetization effects at the sample edges. The estimation of intergrain  $J_c$  in this case can be provided only via the invocation of a suitable critical state model. For this model to be valid, it must include sample geometry and intragrain shielding currents flowing on the grain surface. These multiple factors make the ac induction methods very difficult to apply to ceramic high- $T_c$  samples at low magnetic fields.

In this paper, we show that persistent supercurrents flowing in a superconducting ring provide better alternatives. The magnitude of those currents and their critical value was determined using a contactless magnetic-field measurement method. Persistent current generates a magnetic field above the sample and the value of this current can be derived from the Biot-Savart equation. Persistent supercurrent induced in a ring is a self-sustaining current and therefore is sensitive to any change in the intrinsic resistance of the intergrain junction or to a magnetic-flux motion. The objective of this work was to measure the intergrain critical current as a function of temperature and magnetic field for a pure ceramic YBCO and a YBCO-Ag composite in an attempt to reveal the intrinsic character of grain boundaries. Measurements of sample response to an applied magnetic field were performed in order to determine changes in the transport intergrain current caused by the intergrain magnetic-flux trapping and depinning. Studies of both the critical currents and flux motion were done on the samples using the same magnetic measurement tech-

nique, the scanning cryogenic Hall probe. The ring-shaped samples made of a pure ceramic  $\text{YBa}_2\text{Cu}_3\text{O}_{7-\delta}$ , and a 2-wt. % Ag-doped  $\text{YBa}_2\text{Cu}_3\text{O}_{7-\delta}$  ceramic composite were investigated. The results obtained allowed for better understanding of the transport and magnetic properties of intergrain junctions in ceramic YBCO and ceramic YBCO-Ag composites. The results also provided a strong evidence for an intergrain flux-creep controlled transport current.

## II. EXPERIMENTAL PROCEDURES

Different procedures were applied to measure the dependence of intergrain critical current  $I_c$  on temperature over a range of 60-90 K (for various magnetic fields between 0 and 100 G) and on magnetic field over a range of 0-100 G (for various temperatures between 60 and 90 K). The leading idea of this experiment was to measure the critical value of a persistent current induced in a superconducting ring. An induction of a persistent current requires a magnetic flux to be present in the ring central hole. The easiest way to do that is to apply an external magnetic field to the ring above  $T_c$ , cool it in a field down to a certain temperature below  $T_c$  and then remove the external field. However, the magnetic flux trapped in this ring is a combination of a flux supported by the persistent current and a magnetic vortex field trapped in the bulk of the ring. The persistent current leads to a single maximum of the axial component of trapped magnetic field in the center of the ring, whereas, vortices trapped in the bulk of the ring give rise to two maxima near the ring perimeter, and correspondingly to a minimum in the center of the ring.<sup>16,17</sup> Those vortices are of intragrain (Abrikosov) and intergrain (Josephson) nature, and the vortex field is superposed on the field profile generated by the persistent current. In order to avoid the contribution of the vortex field, the measurements of the critical current were performed on ceramic rings containing two parallel narrow constrictions (bridges) and at low applied magnetic fields up to 10-20 G. The bridges allow the creep of magnetic flux from outside into the ring central hole at low magnetic fields and minimize trapping of intergrain vortices in the bulk of the ring. The critical currents were determined in zero-field-cooled (ZFC) and field-cooled (FC) rings.

For the zero-field-cooled case, after cooling the ring down to a certain temperature below  $T_c$ , the external magnetic field (0-20 G) was applied. This was followed by the measurement of the profile of the axial component of the trapped field (supported by the persistent current) when the external field was reduced to zero. The trapped field profiles were studied as a function of the applied magnetic field in order to determine the saturation value of the axial component of the field trapped in the center of the ring [Fig. 1(a)]. That saturation value [Fig. 1(b)] was then used to calculate the intergrain critical current  $I_c$  using the Biot-Savart equation. Saturation of the trapped field normally was achieved by applying magnetic fields up to about 15 G.

In the field-cooled case, the measurement of  $I_c$  was based on the following procedure. After cooling the rings

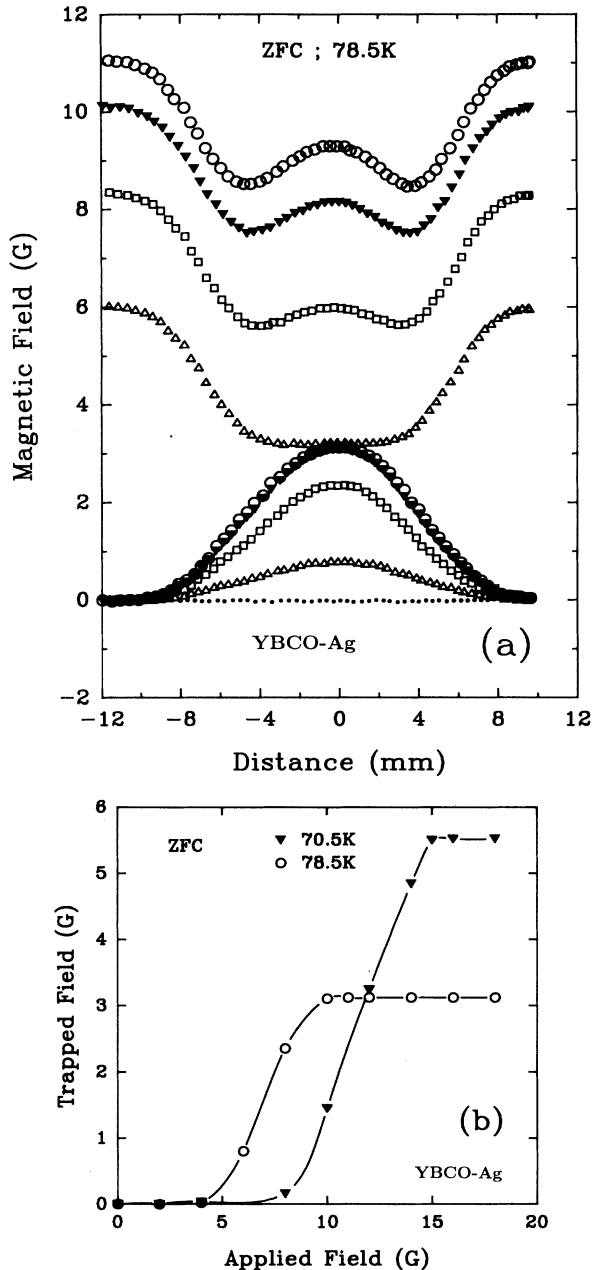


FIG. 1. (a) The profiles of magnetic field measured at 78.5 K by a Hall probe above the zero-field-cooled ring of YBCO-Ag. The upper four curves show the profiles of the diamagnetic shielding measured at applied fields of 6.0, 8.4, 10, and 11 G. Note that the amount of the magnetic flux in the ring's hole increases with the increasing applied field. The corresponding four lower curves represent the magnetic field supported by a persistent current when the external field is reduced to zero. Note that the amount of flux encircled by the current saturates when the current reaches a critical value. The distances +8, -8 mm, and +3, -3 mm mark the ring's outer and inner edges, respectively. (b) The dependence of the magnetic field trapped in the ring's center on applied field, measured at 70.5 and 78.5 K. The magnitude of the trapped field is proportional to the persistent current  $I$  circulating around the ring, and its saturation value is proportional to the intergrain critical current  $I_c$ .

below  $T_c$  in a magnetic field (0–100 G), the additional external magnetic field (0–15 G) was applied. This was followed by the measurement of the axial component of the trapped field profile (supported by the persistent current) when this additional applied field was reduced to zero. In this case, the trapped field was superposed on the Meissner field. Similarly to the zero-field-cooled case, the critical value of the persistent current was determined from the saturation value of the axial component of the field trapped in the ring's center (Fig. 2).

The profiles of the axial magnetic field produced by the persistent current circulating in a superconducting ring were measured across the ring by an axial cryogenic Hall probe (with sensitivity of 20–30 mG at temperatures 60–90 K, and of sensitive area 0.4 mm<sup>2</sup>) over a temperature range of 60–90 K. We did not register any magnetic field generated by the Hall probe at a level of 0.1 mG. The probe was connected to a gaussmeter and a comput-

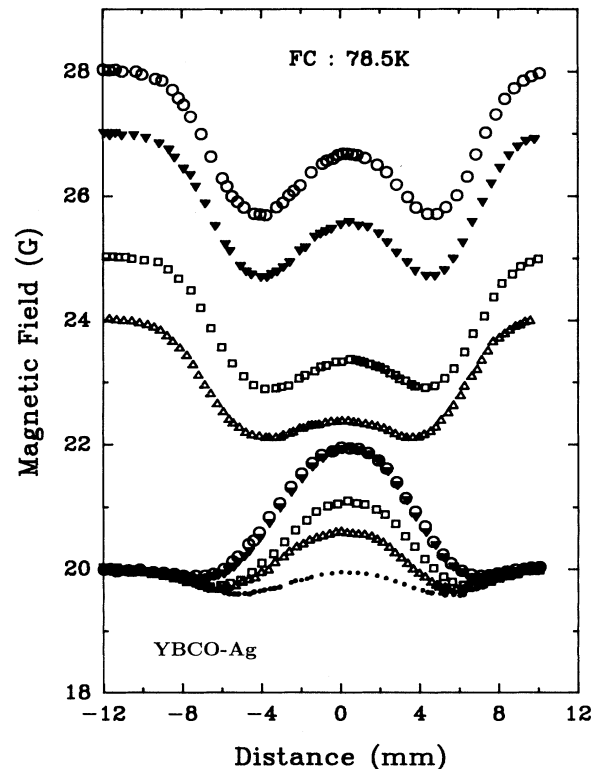


FIG. 2. The profiles of magnetic field measured at 78.5 K by a Hall probe above the YBCO-Ag ring cooled below  $T_c$  in a field of 20 G. The dotted curve shows the profile of the Meissner field at 20 G. The upper four curves show the profiles of that Meissner field superposed on the shielding fields when the additional field of 4, 5, 7, and 8 G was applied to the ring at a temperature of 78.5 K. Note that the amount of the magnetic flux in the ring's hole increases with this additional field. The corresponding four lower curves represent the Meissner field at 20 G superposed on the trapped field that was supported by a persistent current when the additional external field was removed. Note that the saturation value of the trapped field is proportional to the intergrain critical current value at an applied field of 20 G.

er controlled system which allowed the measurements of magnetic-field profiles over a scanning distance of 22 mm and the measurements of fast decays of the magnetic field. A solenoid was used to generate magnetic fields (0–100 G) in a direction perpendicular to the ring plane. The probe measured the component of the magnetic field perpendicular to the plane of the ring-shaped sample at a distance of 1.9–2.0 mm from the ring surface, as measured at room temperature. Variation of that distance with temperature at low temperature (over a range 77–200 K) was tested using a copper wire wound ring-shaped coil instead of the sample. This coil was able to produce magnetic field profiles, similar to those generated by persistent current in a superconducting ring, with the magnitude at the coil's center over a range 0–10 G. It was found that the changes in a magnetic field recorded by the Hall probe were within 0.5–1.0 % of the reading over the whole applied temperature range of 120 K. We studied the dependence of the intergrain critical currents on temperature and magnetic field in the ceramic rings of YBCO and 2-wt. % Ag-doped YBCO composite. Those rings had the outer and inner diameters of 16 and 6 mm, respectively, and were 3.0–3.5 mm thick. Two parallel constrictions (cuts) were made along the ring diameter, forming bridges of the cross-sectional area of about 3.0–3.5 mm<sup>2</sup>. Temperature of the ring was controlled with both a carbon-glass and platinum resistance thermometers and an inductionless foil resistor as a heater.

The material for the ring-shaped samples was prepared from powders of high-purity oxides Y<sub>2</sub>O<sub>3</sub> and CuO, and carbonate BaCO<sub>3</sub> using the standard solid-state reaction technique. The powders were calcined in flowing pure oxygen for 24 h at 925 °C. The resulting product was pulverized and a new disk-shaped pellet was formed under a pressure of about 7000 bar. The disk (16 mm diam, 3.0–3.5 mm thick) was then sintered in flowing oxygen at 925 °C for 7 h and cooled at variable rates down to room temperature (3 °C/min between 925–700 °C and 1 °C/min below 700 °C). In the case of YBCO-Ag composites, silver powder was added to YBCO before the sintering process. After sintering a 6-mm-diam hole was cut in the disk center using a diamond drill sprayed with water. The resulting ring was then cut along its diameter in order to form two bridges of width 1.0–1.5 mm close to the ring inner hole (Fig. 3).

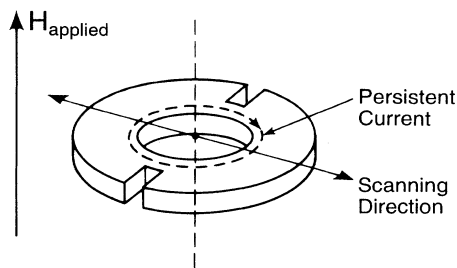


FIG. 3. Schematic picture of the ring's geometry used in the studies of critical current  $I_c$ . Scanning direction denotes the direction of motion of a cryogenic Hall probe across the ring.

### III. EXPERIMENTAL RESULTS

We studied the dependence of the intergrain critical current density on temperature and magnetic field in YBCO and 2-wt. % Ag-doped YBCO continuous ceramic rings. Three kinds of measurements were performed: (1) the dependence of the critical current  $I_c$  on temperature measured in the zero-field-cooled rings, (2) the dependence of the critical current  $I_c$  on temperature measured in the field-cooled rings at constant magnetic field, and (3) the dependence of the critical current  $I_c$  on applied magnetic field measured in the field-cooled-rings at constant temperature. We also investigated dissipation of the persistent current flowing in the rings at various temperatures.

#### A. Dependence of $I_c$ on temperature

Figure 4 presents the dependence of  $I_c$  on temperature over a range of 60–90 K measured in the YBCO continuous ceramic ring for the zero-field cooling and for the field-cooling in magnetic fields of 10, 20, and 30 G. The Hall probe can detect magnetic field generated by a persistent current of magnitude larger than about 10–20 mA. This condition therefore sets the criterion for the “zero resistance”  $T_c^*$  of the intergrain junctions. In the ZFC case,  $T_c^* = 87.5 \text{ K} \pm 0.5 \text{ K}$ , which is about 4 K lower than  $T_c$  of the superconducting grains, determined by dc magnetization measurements. Applied magnetic fields of 10, 20, and 30 G reduce  $T_c^*$  further down to 86.5, 84.5, and 82.5 K ( $\pm 0.5 \text{ K}$ ), respectively, i.e., approximately by 2.0 K per 10 G.

Figure 5 shows the dependence of  $I_c$  on temperature over a range of 60–90 K measured in the continuous ring of 2-wt. % Ag-doped YBCO ceramic composite for the ZFC case and for the field-cooling in magnetic fields of 20, 40, and 60 G.  $T_c^*$  is less sensitive to magnetic field

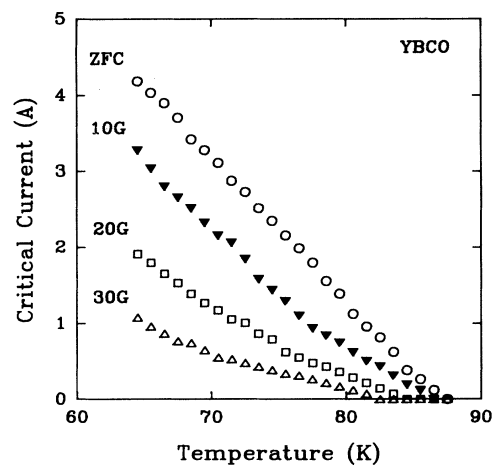


FIG. 4. The dependence of the intergrain critical current  $I_c$  in the YBCO ceramic ring on temperature (over a range between 64 and 87 K) measured for the zero-field cooling (ZFC) and field cooling at 10, 20, and 30 G. Note that the linear dependence of  $I_c$  on temperature close to  $T_c^*$  seen for the ZFC case is preserved at those magnetic fields.

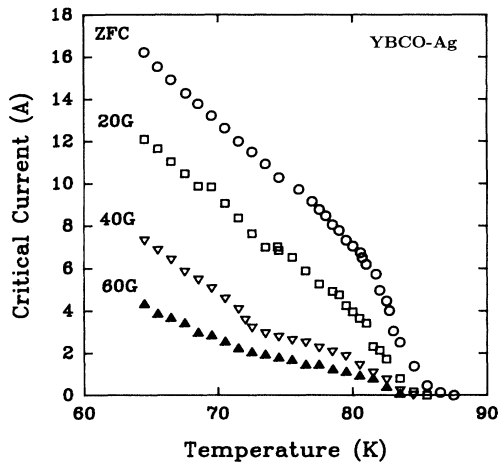


FIG. 5. The dependence of the intergrain critical current  $I_c$  in the 2-wt. % Ag-doped YBCO ring on temperature (over a range between 64–87 K) measured for the zero-field-cooled and field cooled (at 20, 40, and 60 G) samples. Note that the magnetic field modifies the temperature dependence of  $I_c$  close to  $T_c^*$ .

than that for YBCO ceramic ring.  $T_c^*$  decreases from  $86.5 \text{ K} \pm 0.5 \text{ K}$  for the ZFC case down to 85.5, 84.5, and 83.5 K ( $\pm 0.5 \text{ K}$ ) for magnetic fields of 20, 40, and 60 G, respectively, i.e., approximately at a rate of 0.5 K per 10 G.

The intragrain  $T_c$  for those rings equals about  $92.0 \text{ K} \pm 0.5 \text{ K}$  as determined by dc magnetization and resistance measurements as a function of temperature.  $T_c$  is insensitive to small magnetic fields (0–100 G) applied in these studies. Note that the intragrain shielding of the rings can be detected by a Hall probe at temperatures up to about  $90.0 \text{ K} \pm 0.5 \text{ K}$ .

### B. Dependence of $I_c$ on magnetic field

The dependence of the critical current  $I_c$  on magnetic field up to 60–80 G were measured in the YBCO and YBCO-Ag rings at various temperatures between 60 and 90 K. The results are presented in Figs. 6(a) and 6(b). Strong suppression of  $I_c$  with magnetic field is visible at low magnetic fields. At fields higher than a certain value  $H^*$ ,  $I_c$  approaches a constant value.  $H^*$  increases if temperature of the sample is reduced. This behavior is observed as a general trend at temperatures about 5–10 K below  $T_c^*$  in the YBCO and YBCO-Ag rings. However, at temperatures closer to  $T_c^*$ , intergrain transport current in those rings is completely suppressed by magnetic fields of the order of 10–60 G.

### C. Dissipation of persistent current $I$

We measured the dependence of the persistent intergrain current  $I$  flowing in the zero-field-cooled YBCO and 2-wt. % Ag-doped YBCO rings, on time over a range up to  $10^3$  sec at constant temperature and applied magnetic field. In the case of the YBCO ring, we were not able to measure decay in the persistent current because

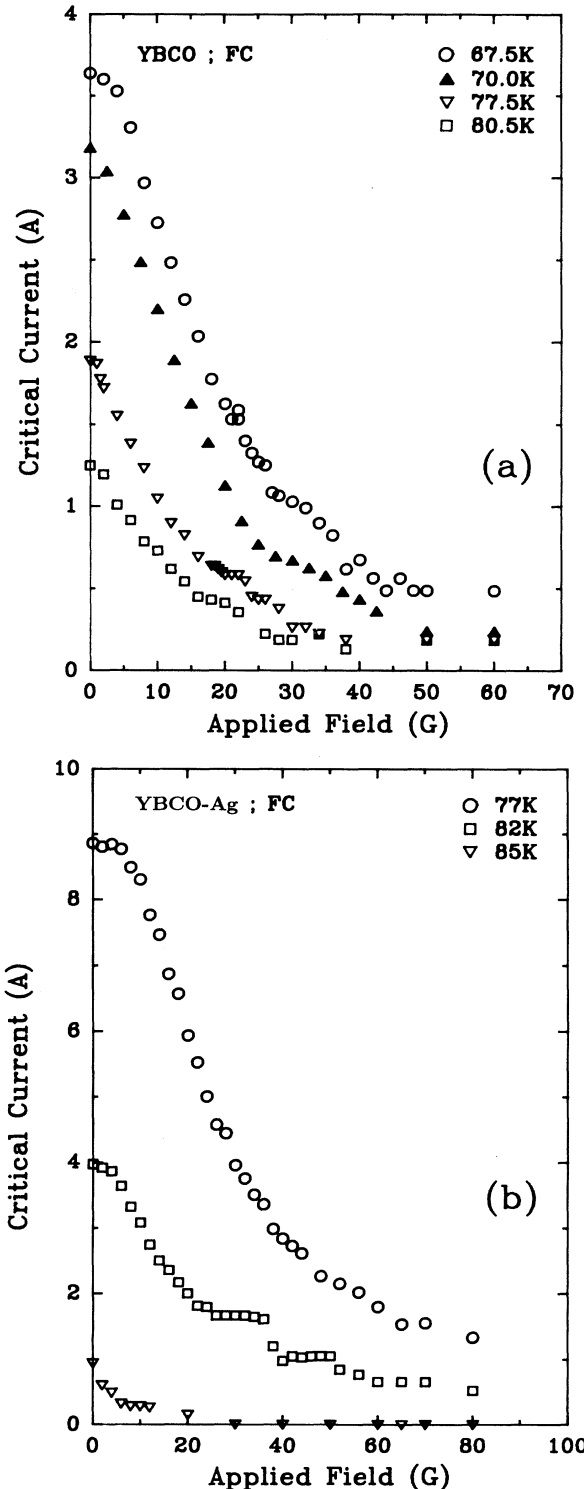


FIG. 6. The dependence of the intergrain critical current  $I_c$  on magnetic field (up to 100 G) measured at various temperatures in the continuous rings of YBCO and 2-wt. % Ag-doped YBCO. (a)  $I_c(H)$  for the YBCO ring measured at a temperature of 67.5, 70.0, 77.5, and 80.5 K. Note the  $\sin H/H$  behavior of  $I_c(H)$  at low fields and a saturation of  $I_c$  at magnetic fields above 35–45 G. (b)  $I_c(H)$  for the 2-wt. % Ag-doped YBCO ring measured at a temperature of 77, 82, and 85 K. The saturation of  $I_c(H)$  occurs at magnetic fields above 60–70 G.

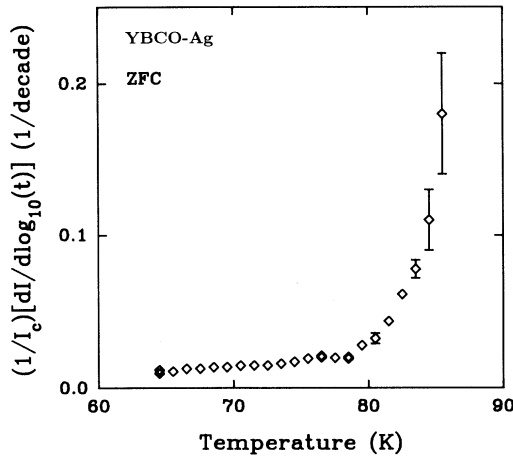


FIG. 7. The dependence of the persistent current decay rate on temperature measured in the zero-field-cooled 2-wt. % Ag-doped YBCO ring. As expected, the decay rates achieve high values at temperatures close to the intergrain  $T_c^* = 86.5$  K.

the system could not detect changes in the current less than about 10 mA per decade, due to the sensitivity limit of the Hall probe used in these studies. However, dissipation of persistent current was observed in the 2-wt. % Ag-doped YBCO ring. The decay rates of the current were measured in the zero-field-cooled sample up to  $10^3$  sec and found to be logarithmic. The decay rate increases with increasing temperature of the sample (Fig. 7) and reaches high values close to  $T_c^*$ . The persistent current decreases down with time from its maximum (critical) value. The current can regain the original value if additional magnetic flux is supplied through the ring's bridges into the ring's central hole. This can be easily done by applying the original external magnetic field to the ring and subsequently reducing its magnitude to zero.

#### IV. DISCUSSION

The experiments presented above provide important information on the intrinsic nature of the intergrain superconducting junctions in YBCO ceramics and YBCO-Ag ceramic composites and on the intergrain flux-creep-controlled transport current in those materials. The measurements of the intergrain critical current on temperature and magnetic field revealed different character of the grain boundaries in pure YBCO ceramics in comparison to those in YBCO-Ag ceramic composites. Decays of the persistent current studied at various temperatures showed that the process of current dissipation is thermally activated.

Since the results obtained were based on the measurement of a true supercurrent, there are several problems related to the microstructure of the grain boundary and its electrical and magnetic properties, that require discussion. The problems that should be considered are as follows:

(1) What model of the grain boundary should be used to describe behavior of  $I_c$  in high- $T_c$  ceramics?

(2) What does the magnetic dependence of  $I_c$  imply about the grain-boundary microstructure?

(3) How does the pinning and motion of magnetic flux at the grain boundaries affect the intergrain transport current?

Ceramic high- $T_c$  superconductors have been modeled by an array of weakly coupled superconducting grains.<sup>18</sup> This model assumes the presence of two superconducting media: the weak links between grains (grain boundaries) and the grains themselves. The critical current  $I_c$  is therefore limited by the intergrain junctions and depends on their intrinsic properties such as the type of junction, its geometry and inhomogeneity.<sup>19</sup> The grain boundary  $I_c$  in YBCO ceramics turned out to be sensitive to the grain misorientation angle<sup>9</sup> (even if the Cu-O planes in the adjacent crystals are essentially parallel), to local variations in structure and/or composition (foreign phases, microprecipitates) and to random variation in the intergrain junction thickness. It was suggested that the weak-link behavior of grain boundaries in YBCO ceramics could be that of a Josephson tunnel (SIS) junction,<sup>1,2,5,20</sup> with the critical current determined by the weakest junction on the current percolative path. For a Josephson junction the dependence of the critical current  $I_{cj}$  on temperature  $T$  is described by the Ambegaokar and Baratoff formula:<sup>21</sup>

$$I_{cj}(T) = \frac{\pi}{2e} \frac{\Delta(T)}{R_N} \tanh \left[ \frac{\Delta(T)}{2kT} \right] \quad (1)$$

for the maximum (dc) Josephson current where  $\Delta$  is the energy gap and  $R_N$  is the tunneling resistance per unit area of the junction when both grains in the normal state.

The magnetic field penetrating the barrier of a Josephson junction reduces the tunneling current. If the junction is rectangular and the field is normal to an edge of length  $L$ , the critical current is described by the Fraunhofer pattern<sup>19</sup>

$$I_{cj}(H) = I_{cj}(0) \left| \frac{\sin(\pi H/H_0)}{\pi H/H_0} \right|, \quad (2)$$

where  $H_0$  is given by

$$H_0 = \frac{\Phi_0}{\mu_0 d L} \quad (3)$$

here  $\Phi_0$  is the flux quantum,  $\mu_0$  is the permeability of free space, and  $d = 2\lambda + t$  is the effective junction thickness,  $\lambda(T)$  being the London penetration depth and  $t$  the barrier thickness.

The Josephson junction coupling strength is defined by the Josephson coupling energy between two grains

$$E_j(T) = \frac{\hbar I_{cj}(T)}{2e}. \quad (4)$$

Close to  $T_c$  the Ambegaokar and Baratoff formula [Eq. (1)] can be approximated by the relation

$$I_{cj}(T) = \text{const}(T_c - T). \quad (5)$$

However, Clem *et al.*<sup>22</sup> revealed that the dependence of

$I_{cj}$  on temperature depends on the ratio between the junction coupling energy  $E_j$  and the condensation energy  $E_c$ ,

$$\varepsilon = \frac{E_j(T)}{E_c(T)}, \quad (6)$$

where  $E_j(T)$  is given by Eq. (4) and  $E_c(T)$  is

$$E_c(T) = \frac{H_c(T)^2}{8\pi V}. \quad (7)$$

Here  $V$  is the volume of a grain and  $H_c$  is the thermodynamical critical field. If  $\varepsilon \ll 1$  (weak-coupling limit) the temperature dependence of  $I_{cj}$  close to  $T_c$  is linear. For  $\varepsilon \gg 1$  (strong-coupling limit)  $I_{cj}$  varies with temperature like the critical current of individual superconducting grains according to the Ginzburg-Landau approach

$$I_{cj}(T) = \text{const}(T_c - T)^{3/2}. \quad (8)$$

Ambegaokar and Halperin<sup>23</sup> pointed out that thermal fluctuations in sufficiently weak Josephson links can lead to a very significant reduction in the zero resistance temperature at which  $I_{cj}=0$ . The energy of a Josephson junction can be represented by the formula:

$$U = -E_J \{ \cos\varphi + [I/I_{cj}(T)]\varphi \}, \quad (9)$$

where  $I$  is the applied current and  $\varphi$  is the superconducting phase difference across the junction. Change in the phase difference  $\varphi$  by  $\pm 2\pi$  results in an energy minimum for the junction. This means that the phase-slip process by  $\pm 2\pi$  can be thermally activated with a barrier height defined by

$$U_0 = 2E_J = \hbar I_{cj}(T)/e, \quad (10)$$

and leads to a nonzero voltage across the junction proportional to the phase-slip rate.

Gross *et al.*<sup>18</sup> and Keene<sup>24</sup> suggested that thermally activated phase slippage can occur in YBCO grain-boundary Josephson junction, causing a reduction of the Josephson coupling energy and a depression of the measured critical temperature of the junction below that of the superconducting grains forming the junction.

If the superconducting grains are separated by a thin layer of normal metal instead of an insulator, the dependence of  $I_{cj}$  flowing through that junction (SNS proximity junction) on temperature can be written in the De Gennes form<sup>25</sup>

$$I_{cj}(T) \propto (T_c - T)^2 \exp[-2d_N/\xi_N(T)], \quad (11)$$

where  $2d_N$  is the metal layer thickness and  $\xi_N(T) \propto T^{-1/2}$  represents the penetration distance of pairs into the normal metal. Close to  $T_c$  this formula can be replaced by a simple expression:

$$I_{cj}(T) = \text{const}(T_c - T)^2. \quad (12)$$

Measurements of  $I_c$  as a function of temperature close to  $T_c$  have been used to determine what type of intergrain junctions exists in YBCO ceramics.

Figure 8 presents the dependence of  $I_c$  on  $1 - T/T_c^*$  for ceramic samples of YBCO and 2-wt. % Ag-doped

YBCO composites. These results were plotted on a logarithmic scale in order to determine the value of  $\alpha$  in the equation  $I_c = \text{const}(1 - T/T_c^*)^\alpha$  for temperatures close to the superconducting transition temperature  $T_c^*$  of the intergrain junction. For the zero-field-cooled YBCO sample  $\alpha = 1.0 \pm 0.1$  [Fig. 8(a)]. Field cooling at 10, 20, and 30 G does not substantially change  $\alpha$ . The estimated value of  $\alpha$  equals  $1.0 \pm 0.1$  at 10 G and  $1.1 \pm 0.1$  at higher fields. The dependence of  $I_c$  on temperature agrees with that represented by Eq. (5) for a Josephson tunnel (SIS) junction. Intergrain junctions in YBCO were found to be oxygen depleted,<sup>26</sup> using electron-energy-loss spectroscopy. The insulating layer between superconducting grains may therefore be formed by an oxygen deficient YBCO. On the other hand, for the zero-field-cooled 2-wt. % Ag-doped YBCO sample  $\alpha = 2.0 \pm 0.2$  [Fig. 8(b)], close to  $T_c^*$

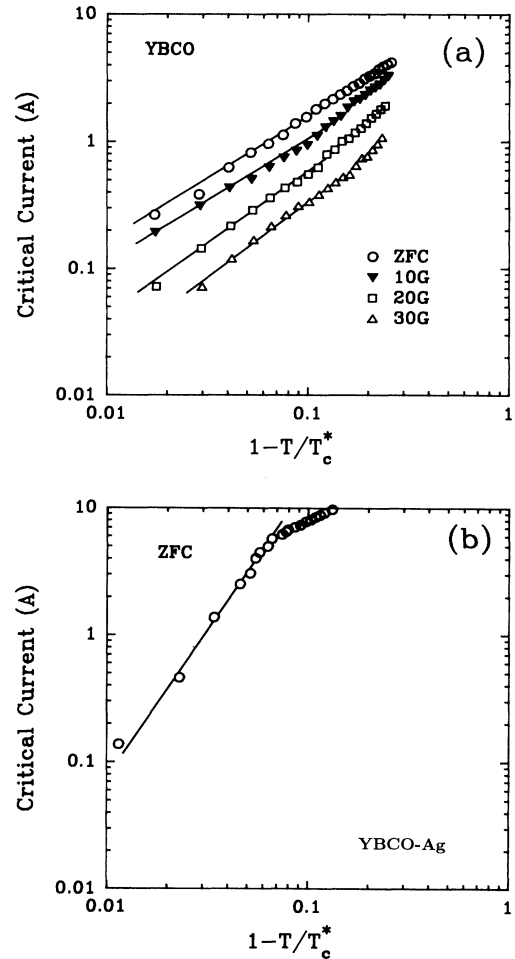


FIG. 8. The dependence of  $I_c$  on the reduced temperature ( $1 - T/T_c^*$ ) plotted for the rings of YBCO and 2-wt. % Ag-doped YBCO, in order to determine the value of  $\alpha$  in the equation  $I_c = \text{const}(1 - T/T_c^*)^\alpha$ . (a) The results for the YBCO ring;  $\alpha = 1.0 \pm 0.1$  for the zero-field cooling and field cooling at 10 G. Field-cooling at 20 and 30 G gives  $\alpha = 1.1 \pm 0.1$ . (b) The results for the 2-wt. % Ag-doped YBCO ring;  $\alpha = 2.0 \pm 0.2$  for zero-field cooling. Field cooling produces random values of  $\alpha$  which may be attributed to the intergrain flux creep in this sample.

and the dependence of  $I_c$  on temperature follows that of Eq. (12) for a proximity (SNS) junction. However, the critical current dependence on temperature measured at magnetic fields of 20, 40, and 60 G revealed that  $\alpha$  assumes random values independent of the applied field. This could be caused by magnetic-flux motion close to  $T_c^*$ .

The dependence of  $I_c$  on magnetic field measured in the YBCO and 2-wt % Ag-doped YBCO rings is presented in Figs. 6(a) and 6(b). The behavior of  $I_c$  for the Josephson junction measured as a function of applied magnetic field resembles a Fraunhofer-like diffraction pattern with minima that correspond to the integral values of flux quantum  $\Phi_0$  [Eq. (2)]. In superconducting ceramics, we deal with multiple grain connections and the geometry of junctions is not uniform across the sample. This means that magnetic flux penetrating the junction will approach  $\Phi_0$  for various magnetic fields depending on the junction geometry. The resulting superposition of currents from various junctions, therefore, will not exhibit oscillations, but possibly a steplike behavior visible in Figs. 6(a) and 6(b).

$I_c(H)$ , measured in the YBCO and YBCO-Ag samples at low magnetic fields, is strongly suppressed by a magnetic field according to Eq. (2). However, at fields higher than certain field  $H^*$ ,  $I_c$  approaches a constant value. This behavior was explained as due to the microstructure of grain boundaries.<sup>4</sup> Conductivity of grain boundaries is believed to arise from two different channels of intergrain conduction. Weak links (Josephson tunnel junctions or proximity junctions) between superconducting grains provide a major channel that occupies about 99.9% of the grain-boundary area available for the current, but cannot carry the supercurrent at high magnetic fields. The second channel is set up by microbridges of intrinsic intragranular material (strong links) across the grain boundaries. Those microbridges occupy less than 0.1% of the grain-boundary area<sup>4</sup> but can carry supercurrent up to very high magnetic fields.

The measurements of persistent current dissipation were completed for the zero-field-cooled ring of 2-wt. % Ag-doped YBCO composite. The decay of current circulating around the ring was found to be logarithmic in time. The logarithmic decay rates, measured as a function of temperature (over a range between 64 and 86 K), are plotted in Fig. 7. They reach higher values at temperatures close to  $T_c^*$ , as expected. The experimental procedure, that was applied to generate a persistent current around the ring, allows for an intergrain flow of magnetic flux from outside the ring into the ring's inner hole. That flux flow occurs through the ring narrow bridges at external magnetic fields up to 10–15 G, and results in flux trapping in the ring's grain boundaries when the applied field is removed. When the current starts to circulate in the ring, the Lorentz force stimulates thermally activated motion of intergrain vortices in the radial direction out of the ring (by reducing the vortex pinning potential). The motion of vortex lines generates an electric field in the direction of the current. It means that the ring offers resistance to the flow of transport current and power is being dissipated in the superconductor. The flux encir-

led by the current in the ring's center will move out into the ring's bulk as soon as fluctuation of the current occurs. Therefore, the observed decay rate of magnetic flux trapped in the ring's hole represents also the relaxation of intergrain-vortex field trapped in the ring's bridges. According to the Anderson's theory of flux creep,<sup>27</sup> the rate at which vortices jump over the pinning barriers is given by

$$v = v_0 \exp(-E/kT), \quad (13)$$

where  $v_0$  is an attempt frequency and  $E$  is an effective activation energy. Thermally activated motion of vortices in a superconducting ring is assisted by the applied driving force, which arises from the macroscopic persistent current of density  $J$  circulating around the ring and is given by the Lorentz-like relation

$$F = B_Z J V, \quad (14)$$

where  $B_Z$  is the local magnetic field in the bulk of the ring, parallel to the ring's axis and  $V$  is the vortex volume. In this case, the effective activation energy  $E$  is a decreasing function of  $F$  and can be represented by<sup>28</sup>

$$E = E_0 - FX = E_0 - B_Z J V X, \quad (15)$$

where  $X$  is the effective geometrical width of the energy barrier,  $E_0$  is presumed to be the height of the energy barrier for thermally activated motion of a vortex, and the term  $FX$  represents the decrease in the height of the barrier due to applied forces.

According to the model of the thermally activated flux motion, the relaxation of the intergrain-vortex field  $H$  trapped in the ring's bridges can be expressed by<sup>29,30</sup>

$$\frac{1}{H(0)} \frac{dH(t)}{d \ln t} = - \frac{kT}{E}, \quad (16)$$

where  $H(0)$  is the initial trapped field, and  $t$  is time. As discussed earlier, the same relaxation rate applies to the dissipation of the persistent current circulating in the ring and the decay of the magnetic flux encircled by this current. The decay rate of the current can be written in agreement with Eq. (16) as

$$\frac{1}{I_c} \frac{dI(t)}{d \ln t} = - \frac{kT}{E}. \quad (17)$$

Figure 7 presents the values of the persistent current decay rates measured as a function of temperature in the zero-field-cooled 2-wt. % Ag-doped YBCO ring. Those values were then used to calculate the dependence of effective activation energy  $E$  on temperature (Fig. 9).  $E$  varies between about 1.2 and 0.1 eV for a temperature range between 64–85 K (at 77 K,  $E \approx 0.8$  eV).

It is noticeable that the  $E(T)$  curve resembles the  $I_c(T)$  one in Fig. 5, taken for the zero-field-cooled ring of 2-wt. % Ag-doped YBCO. This suggests that  $E$  could be proportional to  $I_c$ . Such possibility was considered by Mee *et al.*,<sup>31</sup> while analyzing the thermally activated motion of magnetic flux lines through a network of superconducting grains connected by Josephson junctions. A relation between the critical current density and the logarithmic flux-creep rate was derived for this model, assum-



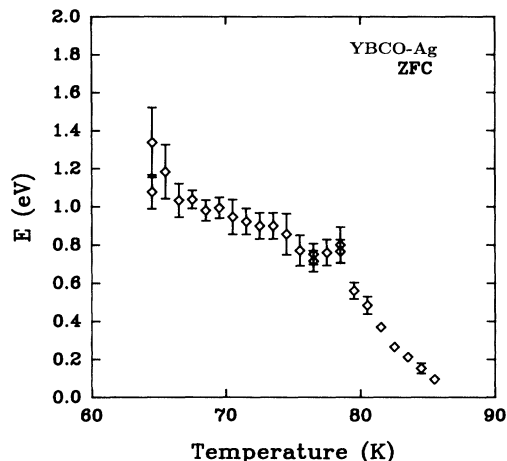


FIG. 9. The dependence of the effective activation energy  $E$  for the intergrain flux creep (and the persistent current dissipation) on temperature (over a range between 64 and 86 K) calculated [Eq. (17)] for the zero-field-cooled ring of 2-wt. % Ag-doped YBCO composite. Note a resemblance of this dependence to that of  $I_c$  on temperature measured in the zero-field-cooled sample (Fig. 5).

ing that the potential barriers for the intergrain flux motion arise from the differences between the maxima and minima of the Josephson junction energy  $U$  [Eq. (9)], and that there are linear relationships between the energies of the barrier and the junction critical current. The above considerations apply also to proximity junctions. According to DeGennes<sup>25</sup> the current-phase and energy-phase relationships for a proximity SNS junction are similar to those for a tunnel SIS junction. The difference between the tunnel and proximity case lies in the behavior of the pair potential within the junction. For an SIS junction the pair potential is the same as that in the bulk superconducting material. However, the pair potential within an SNS junction is much smaller than that in the bulk.

We calculated the ratio between the total coupling energy defined as  $E_{JT} = \hbar I_c / (2e)$  and the activation energy  $E$  (Fig. 9). The values of  $E_{JT}/E$  plotted as a function of temperature in Fig. 10 exhibit a weak temperature dependence and oscillate around a fixed value represented by a straight dotted line. This systematic oscillation of the data points at temperatures close to  $T_c^*$  could be caused by the dependence of the  $\cos\varphi$  term on temperature in the formula for the junction energy [Eq. (9)]. The  $\cos\varphi = f(T)$  problem was intensively studied during the seventies in conventional superconductors. Substantial variation of the  $\cos\varphi$  term was observed in Sn-O-Sn Josephson tunnel junctions at temperatures close to  $T_c^*$ .<sup>32</sup>

We attempted to estimate the intergrain junction critical currents  $I_{cj}$  in 2-wt. % Ag-doped YBCO composite taking  $E_j$  [Eq. (4)] equal to  $E$ . The average  $I_{cj}$  equals about 0.45 mA at a temperature of 64 K.  $I_{cj}$  decreases down with increasing temperature and reaches a value of about 0.05 mA at 85 K.

The essential question that remained is why the total

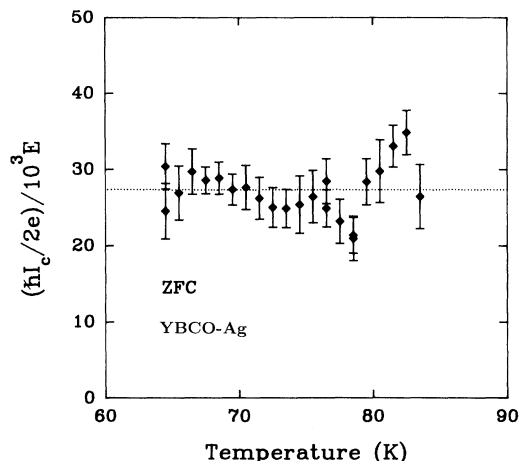


FIG. 10. The ratio between the total coupling energy  $E_j = \hbar I_c(T) / (2e)$  and the effective activation energy for the intergrain flux creep  $E$ , plotted as a function of temperature (a range between 64 and 86 K) for the zero-field-cooled 2-wt. % Ag-doped YBCO ring. Note the systematic scattering around a certain constant value which could be caused by the dependence of the  $\cos\varphi$  in Eq. (9) on temperature.

critical current in 2-wt. % Ag-doped YBCO composite achieves such high values (about 4 times higher than in YBCO at 64 K; the ZFC case) but the activation energy for the thermal dissipation of the current is so low. For comparison, rough estimation of the lower limit of the activation energy in the zero-field-cooled YBCO ring gives values of about 3 and 5 eV for temperatures of 77 and 64 K, respectively. High total critical currents in 2-wt. % Ag-doped YBCO should not implicate, in this case, a high critical current density  $J_{cT}$ . This is a surprising result. It means that the intergrain critical current density  $J_{cT}$  in YBCO-Ag composite is actually less than that in YBCO.

The role that silver plays in YBCO-Ag composites is still not completely clear. It was previously reported that the presence of silver in the intergranular space of ceramic YBCO enhances critical current density  $J_{cT}$  through intergrain junctions usually by a factor of 2–3 at 77 K and zero applied magnetic field for a substitution level over a range of 3–10 wt. %.<sup>33–35</sup> The results of this work show that  $J_{cT}$  in 2-wt. % Ag-doped YBCO has lower values than that of YBCO (due to low activation energy for thermal dissipation of current). Low  $J_{cT}$  means low pinning energy of intergrain magnetic flux in this composite. Therefore, the observed high total critical current in 2-wt. % Ag-doped YBCO must be a consequence of a large effective area of a grain boundary available for the supercurrent conduction. Grain boundaries in YBCO ceramics are known to transmit supercurrent through narrow channels<sup>36</sup> and therefore, they limit the supercurrent carrying capacity of YBCO ceramics in spite of the higher  $J_{cT}$  (higher pinning energy of intergrain flux) than that in 2-wt. % Ag-doped YBCO.

The effect of silver on transport properties of YBCO ceramics is believed to arise from a modification of sinter-

ing conditions [by reducing the melting temperature of YBCO (Refs. 37 and 38)], which creates a uniform grain-size distribution,<sup>34</sup> and from a silver-induced modification of the intrinsic properties of grain boundaries. Related to that is the question whether silver coats grain boundaries as suggested by Weinberger *et al.*<sup>34</sup> or it facilitates oxygenation of intergrain junctions during the sintering process as suggested by Goyal, Burns, and Funkenbusch.<sup>39</sup> Our investigation confirmed that the addition of silver into YBCO leads to transformation of SIS-type junctions into SNS ones, and to a reduction in the pinning potential of the intergranular flux. The sintering conditions of YBCO+Ag produce better intergrain electrical contact, which results in higher magnitude of supercurrent that can flow through a cross-sectional area of a superconducting ceramic, however, the shortage of strong pinning centers for the intergrain flux is the reason for the observed dissipation of the intergrain critical current.

### V. CONCLUSIONS

In order to study the electromagnetic properties of grain boundaries in YBCO ceramics and its composites (including the effect of intergrain flux creep on intergrain transport currents), two important experimental conditions must be satisfied. The supercurrent used to probe the grain boundaries must be a self-sustaining one so it is sensitive to any resistive dissipation. On the other hand, its properties must be measured using a contactless method. The experimental setup used to fulfill that requirement, uses persistent supercurrents induced in superconducting ceramic rings and a Hall probe to detect the critical values of that current and its dissipation rates. The following important information was obtained using this method:

(1) The dependence of  $I_c$  on temperature close to  $T_c^*$  confirms that the intergrain junctions in YBCO behave like SIS-type tunnel junctions [ $I_c = \text{const}(1 - T/T_c^*)$ ] and that the grain boundaries in YBCO-Ag composites have characteristics of SNS-type proximity junctions [ $I_c = \text{const}(1 - T/T_c^*)^2$ ]. In YBCO, this behavior does not change with magnetic field, however, it is affected by the field in the YBCO-Ag composite, suggesting the influence of flux pinning on critical currents. The suppression of the intergrain junction  $T_c^*$  by magnetic field in YBCO-Ag is smaller than the corresponding change in  $T_c^*$  for YBCO.

(2)  $T_c^*$  of the intergrain junctions was found to be about 5 K lower than the intragrain  $T_c$  and about 4 K lower than the zero resistance  $T_c$  determined from a four-probe  $I$ - $V$  measurements (Fig. 11). This means that the  $I$ - $V$  method generally overestimates  $I_c$  and may affect the temperature dependence of  $I_c$  close to  $T_c$ .

(3) The dependence of  $I_c$  on applied magnetic field  $H$  shows, as expected, the  $\sin H/H$  behavior at low magnet-

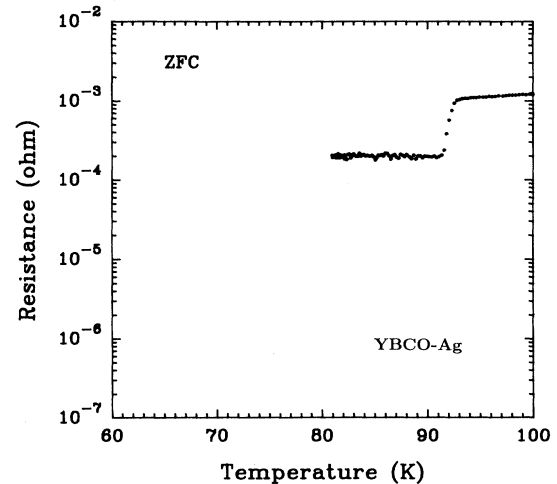


FIG. 11. The resistance of the zero-field-cooled 2-wt. % Ag-doped YBCO ring-shaped sample measured as a function of temperature (over a range between 77 and 295 K) using the  $I$ - $V$  four-probe technique. A constant current source supplying a current of 10–100 mA and nanovoltmeter of a noise level 20 nV has been used in this experiment. The lack of sensitivity inherited in this technique prevented the measurement of the low level resistance and gave a false indication that the intergrain zero resistance  $T_c$  is about 91.0 K  $\pm$  0.5 K. Note that the YBCO-Ag ring cannot support a persistent current of 10–100 mA at temperatures above 86.5 K  $\pm$  0.5 K.

ic fields for all rings. For YBCO and YBCO-Ag rings,  $I_c$  approaches a constant value at higher fields, which may be an indication of the presence of microbridges of intrinsic material across grain boundaries.

(4) Studies of the decay rates of persistent current flowing in the zero-field-cooled superconducting ring of YBCO-Ag provided strong evidence for intergrain flux-creep-controlled transport current. The calculated activation energy for intergrain flux creep is roughly proportional to the initial value of the intergrain critical current  $I_c$  over a range of temperatures between 64 and 83 K. In spite of the lower activation energy, the results show higher total critical currents in 2-wt. % Ag-doped composite than in YBCO. This suggests that intergrain  $J_{cT}$  in the YBCO-Ag composite is actually lower than that in YBCO and the observed higher total critical current  $I_c$  in YBCO-Ag is due to a larger surface area of grain-boundary conduction in this composite.

### ACKNOWLEDGMENT

This work was supported by grants from the Natural Sciences and Engineering Research Council of Canada (NSERC).

<sup>1</sup>J. F. Kwak, E. L. Venturini, D. S. Ginley, and W. Fu, in *Novel Superconductivity*, edited by S. A. Wolf and V. Z. Kresin (Plenum, New York, 1987), p. 983.

<sup>2</sup>J. F. Kwak, E. L. Venturini, P. J. Nigrey, and D. S. Ginley,

Phys. Rev. B **37**, 9749 (1988).

<sup>3</sup>H. Dersch and G. Blatter, Phys. Rev. B **38**, 11 391 (1988).

<sup>4</sup>J. W. Ekin, H. R. Hart, Jr., and A. R. Gaddipati, J. Appl. Phys. **68**, 2285 (1990).

- <sup>5</sup>R. L. Peterson and J. W. Ekin, *Phys. Rev. B* **37**, 9848 (1988).
- <sup>6</sup>P. Chaudhari, J. Mannhart, D. Dimos, C. C. Tsuei, J. Chi, M. M. Oprysko, and M. Scheuermann, *Phys. Rev. Lett.* **60**, 1653 (1988).
- <sup>7</sup>J. Mannhart, P. Chaudhari, D. Dimos, C. C. Tsuei, and T. R. McGuire, *Phys. Rev. Lett.* **61**, 2476 (1988).
- <sup>8</sup>R. Gross, P. Chaudhari, D. Dimos, A. Gupta, and G. Koren, *Phys. Rev. Lett.* **64**, 228 (1990).
- <sup>9</sup>D. Dimos, P. Chaudhari, and J. Mannhart, *Phys. Rev. B* **41**, 4038 (1990).
- <sup>10</sup>X. Yu and M. Sayer, *Phys. Rev. B* **44**, 2348 (1991).
- <sup>11</sup>K. H. Müller, D. N. Matthews, and R. Driver, *Physica C* **191**, 339 (1992).
- <sup>12</sup>W. Paul and Th. Baumann, *Physica C* **175**, 102 (1991).
- <sup>13</sup>N. Ohtani, E. S. Otabe, T. Matsushita, and B. Ni, *Jpn. J. Appl. Phys.* **31**, L169 (1992).
- <sup>14</sup>M. Forsthuber, R. Schneeweiss, G. Hilscher, and F. Gömöry, *Supercond. Sci. Technol.* **5**, S137 (1992).
- <sup>15</sup>C. P. Bean, *Phys. Rev. Lett.* **8**, 250 (1963).
- <sup>16</sup>P. Leiderer and R. Feile, *Z. Phys. B* **70**, 141 (1988).
- <sup>17</sup>M. A.-K. Mohamed and J. Jung, *Phys. Rev. B* **70**, 4512 (1991).
- <sup>18</sup>J. R. Clem, *Physica C* **153-155**, 50 (1988).
- <sup>19</sup>A. Barone and G. Paterno, *Physics and Applications of the Josephson Effect* (Wiley, New York, 1982).
- <sup>20</sup>R. L. Peterson and J. W. Ekin, *Physica C* **157**, 325 (1989).
- <sup>21</sup>V. Ambegaokar and A. Baratoff, *Phys. Rev. Lett.* **10**, 486 (1963).
- <sup>22</sup>J. R. Clem, B. Bumble, S. I. Raider, W. J. Gallagher, and Y. C. Shih, *Phys. Rev. B* **35**, 6637 (1987).
- <sup>23</sup>V. Ambegaokar and B. I. Halperin, *Phys. Rev. Lett.* **22**, 1364 (1969).
- <sup>24</sup>M. N. Keene, *Supercond. Sci. Technol.* **3**, 312 (1990).
- <sup>25</sup>P. G. DeGennes, *Rev. Mod. Phys.* **36**, 225 (1964).
- <sup>26</sup>S. E. Babcock (unpublished).
- <sup>27</sup>P. W. Anderson, *Phys. Rev. Lett.* **9**, 309 (1962).
- <sup>28</sup>P. W. Anderson and Y. B. Kim, *Rev. Mod. Phys.* **36**, 39 (1964).
- <sup>29</sup>A. M. Campbell and J. E. Evetts, *J. Appl. Phys.* **21**, 199 (1972).
- <sup>30</sup>M. R. Beasley, R. Labusch, and W. W. Webb, *Phys. Rev.* **181**, 682 (1969).
- <sup>31</sup>C. Mee, A. I. M. Rae, W. F. Vinen, and C. E. Gough, *Phys. Rev. B* **43**, 2946 (1991).
- <sup>32</sup>O. H. Soerensen, J. Mygind, and N. F. Pedersen, *Phys. Rev. Lett.* **39**, 1018 (1977).
- <sup>33</sup>B. Dwir, M. Affronte, and D. Pavuna, *Appl. Phys. Lett.* **55**, 399 (1989).
- <sup>34</sup>B. R. Weinberger, L. Lynds, D. M. Potrepka, D. B. Snow, C. T. Burila, H. E. Eaton, Jr., R. Cipolli, Z. Tan, and J. I. Budnick, *Physica C* **161**, 91 (1989).
- <sup>35</sup>J. Jung, M. A.-K. Mohamed, S. C. Cheng, and J. P. Franck, *Phys. Rev. B* **42**, 6181 (1990).
- <sup>36</sup>R. A. Buhrman (unpublished).
- <sup>37</sup>T. H. Tiefel, S. Jin, R. C. Sherwood, M. E. Davis, G. W. Kammlott, P. K. Gallagher, D. W. Johnson, Jr., R. A. Fastnacht, and W. W. Rhodes, *Mater. Lett.* **7**, 363 (1989).
- <sup>38</sup>S. Baliga and A. L. Jain, *Appl. Phys. A* **49**, 139 (1989).
- <sup>39</sup>A. Goyal, S. J. Burns, and P. D. Funkenbusch, *Physica C* **168**, 405 (1990).